Mon. Not. R. Astron. Soc. **000**, 1–?? (2002) Printed 2 May 2018 (MN LATEX style file v2.2)

The SLUGGS survey: inferring the formation epochs of metal-poor and metal-rich globular clusters

Duncan A. Forbes[1⋆], Nicola Pastorello[1], Aaron J. Romanowsky[2,3], Christopher Usher[1]
Jean P. Brodie[3], Jay Strader[4]
[1] *Centre for Astrophysics & Supercomputing, Swinburne University, Hawthorn VIC 3122, Australia*
[2] *Department of Physics and Astronomy, San José State University, One Washington Square, San Jose, CA 95192, USA*
[3] *University of California Observatories, 1156 High Street, Santa Cruz CA 95064, USA*
[4] *Department of Physics and Astronomy, Michigan State University, East Lansing, Michigan 48824, USA*

2 May 2018

ABSTRACT

We present a novel, observationally-based framework for the formation epochs and sites of globular clusters (GCs) in a cosmological context. Measuring directly the mean ages of the metal-poor and metal-rich GC subpopulations in our own Galaxy, and in other galaxies, is observationally challenging. Here we apply an alternative approach ulitizing the property that the galaxy mass-metallicity relation is a strong function of redshift (or look-back age) but is relatively insensitive to galaxy mass for massive galaxies. Assuming that GCs follow galaxy mass-metallicity relations that evolve with redshift, one can estimate the mean formation epochs of the two GC subpopulations by knowing their mean metallicities and the growth in host galaxy mass with redshift. Recently, the SLUGGS survey has measured the spectroscopic metallicities for over 1000 GCs in a dozen massive early-type galaxies. Here we use these measurements, and our new metallicity matching method, to infer a mean age for metal-rich GCs of 11.5 Gyr (z = 2.9) and a range of 12.2 to 12.8 Gyr ($4.8 < z < 5.9$) for the metal-poor GCs, depending on whether they mostly formed in accreted satellites or in-situ within the main host galaxy. We compare our values to direct age measurements for Milky Way GCs and predictions from cosmological models. Our findings suggest that reionisation preceded most GC formation, and that it is unlikely to be the cause of GC bimodal metallicity distributions.

Key words: galaxies: star clusters – galaxies: evolution

1 INTRODUCTION

Despite the discovery of multiple stellar populations in Milky Way globular clusters (GCs), they are still dominated by a single old age population with very little variation in the main sequence turnoff age (e.g. Piotto et al. 2007). In this sense they can still be regarded as simple stellar populations that provide a 'fossil record' of star cluster formation at the earliest epochs (see Brodie & Strader 2006 for a review). A key aspect of interpreting this fossil record is the comparison to simulations of GC formation within a cosmological context.

Cosmological simulations are now available that model the formation of the two subpopulations of GCs commonly seen around large galaxies. Although the two subpopulations are observed to have some similar properties (e.g. their mass functions and sizes, to first order), they also differ strongly in others (e.g. their metallicity, spatial distribution and kinematics). These differences point to different epochs and/or locations for their formation. The two subpopulations are commonly denoted by their relative metallicities or colours, i.e. metal-poor/blue and metal-rich/red (Peng et al. 2006; Usher et al. 2012). The exact division in metallicity varies from galaxy to galaxy. Here we refer to two subpopulations as MPGCs and MRGCs.

In this paper we briefly review predictions for the redshift of formation of these two GC subpopulations in recent cosmological models. We also summarise the current situation regarding direct age measurements of the Milky Way's GC subpopulations, and age estimates for extragalactic GCs based on integrated spectra. We then utilise new spectroscopic metallicities, obtained using the Keck telescope, for a

⋆ E-mail: dforbes@swin.edu.au

large sample of GCs from the SAGES Legacy Unifying Globulars and GalaxieS (SLUGGS) survey (sluggs.swin.edu.au; Brodie et al. 2014) and a galaxy mass-metallicity relation that evolves with redshift to estimate the mean formation epoch of GCs in a sample of massive early-type galaxies. This method provides an alternative approach to estimating the mean ages of the two GC subpopulations. We take advantage of the fact that large numbers of GC metallicities from integrated spectra are now available from the SLUGGS survey (Usher et al. 2012, 2015), and that the mass-metallicity relation is a strong function of redshift (i.e. formation epoch) but is rather insensitive to mass for massive galaxies.

2 COSMOLOGICAL MODEL PREDICTIONS FOR GLOBULAR CLUSTER AGES

One of the first cosmological models to predict the formation epoch of the two GC subpopulations was Beasley et al. (2002). Their semi-analytical model formed MPGCs in low mass galaxies and MRGCs in a later gaseous phase but they needed to truncate the formation of MPGCs at z > 5 in order to reproduce the (bimodal) metallicity distribution observed in present day GC systems. Cosmic reionisation was identified as the possible process that would interrupt GC formation. Using Bennett et al. (2014) cosmological parameters, their model predicts mean ages of 12.7 Gyr and 10.2 Gyr for the MPGC and MRGCs respectively in high mass ellipticals (with slightly younger ages for the MRGCs in lower mass host galaxies and/or low density environments).

In the following discussion we assume the redshift as given in the original work and quote a look-back time assuming Bennett et al. (2014) cosmology (i.e. $H_0 = 69.6$, $\Omega_M = 0.286$, $\Omega_{vac} = 0.714$). We use the online calculator of Wright (2006) which gives the age of a flat Universe in this cosmology of 13.72 Gyr.

In the Santos (2003) model, MPGCs also form prior to reionisation at z $\geqslant$ 7 (ages $\geqslant$ 13.0 Gyr) with reionisation expicitly suppressing any further GC formation until it ended. After $\leqslant$ 1.5 Gyrs, the next generation of GCs that form were metal enriched.

In the cosmological simulations of Bekki et al. (2008), GCs form in strong star formation episodes over a large range of redshift. The mean formation epoch of MPGCs is z = 5.7 (12.7 Gyr) and z= 4.3 (12.3 Gyr) for MRGCs.

Griffen et al. (2010) used the Aquarius simulation to resolve the dark matter minihalos which they associated with MPGC formation. In their model, the formation of MPGC was truncated by ionisation from the first-formed GCs. They predict MPGC formation to begin around z = 22 (13.6 Gyr) and end by z = 13 (13.4 Gyr). Their favoured formation for MRGCs is in gaseous major mergers, which give rise to a broad range of ages, i.e. 7–13.3 Gyrs.

Tonini (2013) modelled the hierarchical assembly of galaxies using a Monte Carlo technique. In her model MPGCs form in low mass satellites at z $\sim$ 3–4 (11.5–12.2 Gyr), with MRGCs forming later in a dissipative phase within the main galaxy at z $\sim$ 2 (10.4 Gyr). Both GC subpopulations are imprinted with a metallicity given by the galaxy mass-metallicity relation at that redshift. The satellites are accreted between redshift 4 and 0, with the accretion rate based on the Millennium cosmological simulation (Springel et al. 2005). If the satellite has MRGCs, they are still relatively metal-poor compared to the larger main galaxy. In the case of gas-rich satellites, some new GCs may form and give rise to an intermediate metallicity GC subpopulation. However, observationally such intermediate metallicity peaks in well-studied GC systems are quite rare (Peng et al. 2006).

Based on the earlier cosmological model of Muratov & Gnedin (2010), Li & Gnedin (2014) focused on modelling the GC systems of early-type galaxies in the Virgo cluster. In their model GCs form in gas-rich mergers, with early (minor) mergers leading to mostly MPGCs and later (major) mergers favouring the formation of MRGCs. Like Tonini (2013), the resulting GC metallicities are driven by an evolving galaxy mass-metallicity relation. Thus a single mechanism produces differences in the GC metallicity and age distributions. They predict MPGCs to form at redshifts z = 4–6 (12.2–12.8 Gyr) with MRGCs peaking around z = 3–4 but continuing until z $\sim$ 1 (7.8 Gyr). Thus the MRGCs could be from zero up to 5 Gyr younger than their MPGC counterparts.

Building on the method of Moore et al. (2006) and Spitler et al. (2012), Corbett Moran et al. (2014) associated MPGCs with rare, overdense peaks which collapse early in the Universe. In particular, they modelled the formation of MPGCs in a Virgo cluster like environment, finding a formation redshift that best matches the observed distribution of MPGCs around M87 of z $\sim$ 9 (13.1 Gyr). Like several other studies, they invoked reionisation to ultimately truncate MPGC formation.

Trenti, Padoan & Jiminez (2015) have proposed that MPGCs form in the merger of gas-rich dark matter minihalos (similar to earlier works of Bromm & Clarke 2002 and Boley et al. 2009). These minihalos are later stripped of their dark matter via tidal interactions within the main galaxy halo. They predict a mean formation redshift for MPGCs of z = 9.3 (13.2 Gyr). MRGCs are formed later in mergers between minihalos but a prediction for their mean age is not given.

Focusing on a Milky-Way type galaxy in the Via Lactea II simulation, Katz & Ricotti (2014) found that the MPGCs are dominated by those accreted from satellites but there is also a contribution from MPGCs formed in-situ. The reverse is true of MRGCs, which mostly form in-situ but have an accreted component. In the case of the Milky Way, they predict that over half of the existing GC system was accreted. Their favoured model predicts MPGC formation to occur at z = 7–12 (13.0–13.4 Gyr) and z $\sim$ 2 (10.4 Gyr) for the MRGCs, with the bulk of GC accretion at redshifts less than 4.

As discussed above, the various cosmological models make predictions for the formation epoch and therefore the ages of the MPGC and MRGC subpopulations. Next we briefly review the observational studies of GC ages.

3 OBSERVATIONAL CONSTRAINTS ON GLOBULAR CLUSTER AGES

Determining the absolute age of Milky Way GCs from their colour magnitude diagrams (CMDs) has proved problem-

atic over the years due to uncertainties in stellar evolutionary models, intrinsic abundance variations, foreground dust corrections, helium content and the assumed distance. Nevertheless, studies fitting the main sequence turnoff (MSTO) in deep HST CMDs have converged on an age for the oldest MPGCs of 12.5 Gyr (VandenBerg et al. 2013) to 12.8 Gyr (Marin-Franch et al. 2009). Excluding the clearly younger MRGCs that have a different age-metallicity relation and can be associated with accretion events (Forbes & Bridges 2010), the MRGCs are either roughly coeval with the MPGCs (Marin-Franch et al. 2009) or systematically younger by 1.5 Gyr with a mean age of 11.0 Gyr (Vandenbergh et al. (2013) .

Measuring the age of Milky Way GCs from the luminosity fading (i.e. cooling) sequence of white dwarfs offers an alternative method of obtaining absolute ages that is less sensitive to metallicity than MSTO-based methods. To date less than half a dozen GCs have published white dwarf cooling track ages. They include the metal-poor GC M4 for which Bedin et al. (2009) measured an age of 11.6 Gyr. They estimated a measurement error of $\pm$ 0.6 Gyr but noted that the model uncertainties could be as high as $\pm$ 2 Gyr. More recently, Hansen et al. (2013) applied this method to two other Milky Way GCs. They found a relatively young age of 9.9 $\pm$ 0.7 Gyr for the metal-rich GC 47 Tuc (NGC 104), which is 2.0 $\pm$ 0.5 Gyr younger than their metal-poor GC NGC 6397. However, also using the cooling sequence method but with different models, Garcia-Berro et al. (2014) found an age of 12 Gyr with an uncertainty of $\leqslant$ 1 Gyr for 47 Tuc. Thus the two white dwarf cooling ages for this GC are mutually inconsistent. Using an updated metallicity, Hansen et al. noted that the eclipsing binary V69 in 47 Tuc has an age of 10.39 $\pm$ 0.54 Gyr – this age and uncertainty being consistent with both the Hansen et al. and Garcia-Berro et al. values. Clearly a larger sample of bulge and halo GCs need to be studied in this way, and modelling differences reduced, before we can make robust general conclusions about the absolute (or relative) ages of the two subpopulations of GCs in the Milky Way using white dwarf cooling tracks.

Estimating the relative ages of GCs beyond the Local Group requires measurements of the integrated light, with the best method being an analysis of high signal-to-noise optical spectra. The situation for extragalactic GCs is summarised in the review by Brodie & Strader (2006), i.e. the bulk of age-dated GCs are very old (>10 Gyr) with only a small fraction of those observed having young or intermdeiate ages. In the meta-analysis of Strader et al. (2005) it was concluded that the best Keck spectra available could not separate the mean ages of the metal-poor and metal-rich GC subpopulations to better than 1-2 Gyrs. Using spectra from the VLT, Puzia et al. (2005) found hints of a slightly younger mean age for metal-rich GCs but noted that the significance of the result needed verification from larger samples. Spectroscopic studies of GCs tend to be dominated by GCs located in the inner regions of galaxies. The situation regarding the ages of GC subpopulations beyond the Local Group is largely unchanged since 2005.

4 USING THE MASS-METALLICITY RELATION TO CONSTRAIN GLOBULAR CLUSTER AGES

An alternative approach to directly measuring GC ages is to match GC metallicities to the galaxy mass-metallicity relation at different redshifts and hence infer the GC epoch of formation. A key assumption is that the mean metallicity of a GC subpopulation is determined by the same gas that forms the stars within a galaxy. Indeed, we know that a significant fraction of galaxy stars orginally form in star clusters, which are later disrupted (Lada & Lada 2003; Bastian et al. 2013). We can then use the redshift evolution of the galaxy mass-metallicity relation to estimate the formation epoch (and hence their look-back age, thanks to the era of precision cosmology) of MRGC and MPGCs. This method has the advantage of using easier to obtain mean metallicities of extragalactic GCs rather than very challenging direct measurements of their age.

Spitler (2010) used this approach to focus on the mean metallicity of MRGCs compared to those of the host galaxy field stars as a function of galaxy stellar mass (finding a redshift for MRGC formation of z $\sim$ 3.5). Age limits for both MPGC and MRGCs in Virgo galaxies were investigated using a similar method by Spitler et al. (2012). This work gave wide ranges for the epochs of GC formation, i.e. 2 $<$ z $<$ 4 for MRGCs and 7 $<$ z $<$ 10 for MPGCs. Spitler et al. concluded that MPGCs formed well within the epoch of reionisation. However, a major limitation of these works is that the GC metallicities were based on observed broadband colours under the assumption of old ages, and the GC colour to metallicity transformation is known to vary on a galaxy-to-galaxy basis (Usher et al. 2015). If the mean ages are younger than assumed by Spitler then the redshift of formation found by Spitler is an upper limit. Shapiro et al. (2010) employed a similar approach to show that the mean (photometric) metallicity of MRGCs is consistent with the mass-metallicity relation for z $\sim$ 2 star forming turbulent disks.

A better approach is to use mean GC metallicities based on spectroscopy. Until recently this was only possible for small samples of GCs and galaxies. However, Usher et al. (2012, 2015) and Pastorello et al. (2015) have presented spectroscopic metallicities for over 1000 individual extragalactic GCs based on measurements of the Calcium Triplet (CaT) lines from the SLUGGS survey (Brodie et al. 2014). Here we use these measurements to calculate the mean metallicities of the MPGC and MRGC subpopulations for 11 massive (log $M_* > 10.5$ $M_\odot$) galaxies. These are then compared to evolving galaxy mass-stellar metallicity relations to determine the associated redshift and hence the mean formation epoch of the GC subpopulations. We utilise the fact that the relation is a strong function of redshift but depends only weakly on stellar mass for massive galaxies.

In order to define the mean metallicities of the two GC subpopulations we start with photometry, which has the advantage of being available for large numbers of GCs in a given galaxy. The photometry of several GC systems were fit using Gaussian Mixture Modelling (GMM; Muratov & Gnedin (2010) to separate them into two subpopulations in (g–i) colour (see Usher et al. 2012 for details). For the subsample of blue and red GCs with spectra and suffi-

cient S/N, individual GC metallicities are obtained from the CaT absorption lines using the method outlined in Usher et al. (2012), i.e. CaT indices are transformed into total [Z/H] metallicities using the single stellar population models of Vazdekis et al. (2003). They show good agreement with metallicities from the literature with an rms scatter of $\leqslant 0.2$ dex. Here we determine the weighted mean [Z/H] metallicities for these blue and red GC subpopulations of 11 early-type galaxies.

Blue GCs are known to reveal a 'blue tilt' (i.e. becoming more metal-rich with increasing luminosity) for masses above a few 10^6 $M_\odot$ or $M_i < -11.5$. The tilt is generally interpreted as due to self-enrichment (Strader & Smith 2008; Bailin & Harris 2009). Here we only include those blue GCs less luminous than $M_i = -11$. This exercise removes zero to half a dozen GCs per galaxy and changes the mean metallicity in most cases by less than 0.1 dex. There is no evidence for a red tilt, so for the red GCs we make no such correction. The GC data span a large range in galactocentric effective radii (i.e. from $R \approx 0.4$ R_e to $R \approx 18$ R_e) but show only slight negative radial gradients (Pastorello et al. 2015) so we make no correction for radial gradients in GC metallicities.

It is possible that our GC mean metallicities could be impacted by biases in our spectroscopic selection. Since GC selection is based on the identification of the metallicity-dependent CaT feature, low-metallicity GCs may be excluded if the CaT absorption lines in their spectra are very weak. The spectroscopic subsample also has a bias to more luminous GCs than average. However, Pastorello et al. (2015) showed that spectroscopically- and photometrically-identified blue GCs have similar mean metallicities in the five galaxies for which comparable data were available. For the MRGCs, Pastorello et al. found a systematic tendency for the spectroscopic mean metallicity to be lower than the photometric one in a couple of galaxies although this difference is within the error on the mean.

For each galaxy the total stellar mass is taken from Pastorello et al. (2015), which is based on their K-band extinction corrected magnitude from the 2MASS source catalog (Jarrett et al. 2000).

Although the metallicities for the MPGCs and MRGCs of the Milky Way galaxy are typically determined from CMDs, it is interesting to compare them with those for our 11 massive early-type galaxies from integrated spectra. We take the iron abundances ($[Fe/H]$) for 152 Milky Way GCs from the 2010 edition of the Harris (1996) catalogue. For the 45 GCs with α-element abundances ($[\alpha/Fe]$) from Pritzl et al. (2005) we use their quoted value, otherwise we assume a mean value, i.e. $[\alpha/Fe] = 0.3$. The error on this mean value from the 45 GCs in Pritzl et al. is less than ± 0.1 dex. The total metallicities $[Z/H]$ are then obtained from equation 4 of Thomas, Maraston & Bender (2003):

$$[Z/H] = [Fe/H] + 0.94[\alpha/Fe] \quad (1)$$

Using GMM we find that the metallicity distribution of the Milky Way GCs is highly bimodal, with peaks at $[Z/H] = -1.24 \pm 0.04$ and -0.24 ± 0.03 dex for the MPGCs and MRGCs, respectively. The uncertainty in the peak values also comes from the GMM fit. For the total stellar mass of the Milky Way, we assume $M_{\rm MW} = 6.43 \times 10^{10}$ $M_\odot$ (McMillan 2011). We note that although the GC metallicities for the Milky Way and early-type galaxies are derived from different methods (i.e. CMDs vs CaT spectra), systematic differences in the metallicity scale are less than 0.2 dex (Usher et al. 2012).

Table 1. The early-type galaxy sample and the Milky Way. Galaxy name, mean metallicity of the metal-poor and metal-rich globular clusters with the number of globular clusters in each subpopulation, and galaxy stellar mass.

Galaxy (NGC)	MPGC [Z/H] (dex)	N	MRGC [Z/H] (dex)	N	M_* ($M_\odot$)
1023	-1.34 ± 0.10	8	-0.47 ± 0.12	10	8.24×10^{10}
1400	-1.25 ± 0.19	13	-0.50 ± 0.18	11	1.08×10^{11}
1407	-1.23 ± 0.08	70	-0.39 ± 0.05	79	3.13×10^{11}
2768	-1.48 ± 0.14	14	-0.68 ± 0.11	19	1.57×10^{11}
3115	-1.27 ± 0.06	41	-0.14 ± 0.06	47	8.17×10^{10}
4278	-1.45 ± 0.07	46	-0.63 ± 0.05	77	6.79×10^{10}
4365	-1.39 ± 0.12	29	-0.40 ± 0.05	71	2.49×10^{11}
4473	-1.14 ± 0.07	35	-0.12 ± 0.13	11	6.61×10^{10}
4494	-1.16 ± 0.10	23	$+0.06 \pm 0.11$	15	9.12×10^{10}
4649	-1.04 ± 0.06	71	-0.35 ± 0.07	43	2.86×10^{11}
5846	-1.05 ± 0.16	19	-0.37 ± 0.12	16	2.05×10^{11}
MW	-1.24 ± 0.04	109	-0.24 ± 0.03	43	6.43×10^{10}

The mean MPGC and MRGC metallicities and stellar mass for the 11 early-type galaxies and the Milky Way are given in Table 1. We include NGC 4494 but note that it appears to have a trimodal rather than bimodal metallicity distribution (Usher et al. 2012) which may explain its very metal-rich MRGC mean metallicity. Our early-type galaxy sample has a mean stellar mass of log $M_* = 11.2$ with mean metallicities [Z/H] of –1.23 ± 0.03 and –0.39 ± 0.02 for the MPGC and MRGC subpopulations respectively. Thus the MPGC mean metallicity is comparable to that of the Milky Way, but the MRGC subpopulation is somewhat more metal-poor than that of the Milky Way.

5 AN EVOLVING MASS-STELLAR METALLICITY RELATION

In order to define the redshift evolution of the galaxy mass-metallicity relation we follow the approach of Kruijssen (2014). This involves creating a functional form for an evolving mass-metallicity relation based on observations of the *gas* metallicity at z ∼ 0.1 (Tremonti et al. 2004), z ∼ 2 (Erb et al. 2006) and z ∼ 3–4 (Mannucci et al. 2009). We expect the evolving mass-metallicity relation to be well defined up to redshift z = 4 in the coming years with surveys such as MOSDEF (Sanders et al. 2015).

Although there is a wide range of methods for studying gas metallicity in the literature, when a given method is used the mass-metallicity relations generally agree within 0.1 dex (Kewley & Ellison 2008). Gas metallicity traces the current chemical enrichment of a system, whereas the stellar metallicity is an average value over its star formation history. For GCs, the mean stellar metallicity is imprinted at birth and doesn't change with time. So following Shapiro et al. (2010) we further assume that the gas metallicity is equal to the total stellar metallicity, i.e. [O/H] ≈ [Z/H].

In particular, we adopt equation 5 of Kruijssen (2014):

$$[Z/H] \approx [O/H] = -0.59 + 0.24 \log \frac{M_\star}{10^{10}}$$
$$-8.03 \times 10^{-2} \times \left[\log \frac{M_\star}{10^{10}}\right]^2 - 0.2(z-2) + 0.94[\alpha/Fe] \quad (2)$$

where z is the redshift, $M_\star$ is the total stellar mass expressed in $M_\odot$ and the $0.94[\alpha/Fe]$ term converts [Fe/H] to [Z/H] using Eq. 1. We adopt a mean value for $[\alpha/Fe]$ of 0.3 (Pritzl et al. 2005) and note that there is little or no systematic dependence of the ratio on metallicity, i.e. MPGCs and MRGCs have similar $[\alpha/Fe]$ ratios. We also note that the galaxy mass-metallicity relation shows little or no variation with environment up to z = 2 (Kacprzak et al. 2015) and that it has the same slope up to a redshift of at least 6 according to a recent simulation by Ma et al. (2015). As individual GCs are essentially single stellar populations (at least compared to the complex stellar populations of their host galaxies) we can use measurements of their mean (stellar) metallicity to estimate their epoch of formation given knowledge of their host galaxy stellar mass.

6 RESULTS

In Figure 1 we show the mean metallicity (and error on the mean) for the individual MPGC and MRGC subpopulations of our early-type galaxy sample and the Milky Way as a function of host galaxy stellar mass. The galaxy mass-stellar metallicity relation at various redshifts (Eq. 2) is also shown.

The MRGCs reveal more scatter (and have larger error bars) at low galaxy masses towards younger mean formation ages. This scatter, even at a fixed galaxy mass, may imply a range of MRGC formation histories. The Milky Way GC system is well-known to host several intermediate-age metal-rich GCs that may be associated with accreted satellite galaxies (Forbes & Bridges 2010); a similar situation may be present in low mass early-type galaxies. We note that the stellar mass plotted for the Milky Way is the total mass, whereas MRGCs are mostly associated with the bulge which has a much lower stellar mass of $\sim 10^{10}$ $M_\odot$. The MPGCs in our sample reveal less scatter in their mean metallicities than the MRGCs, suggesting more uniformly old formation ages. For their *current* host galaxy stellar masses, the MRGCs and MPGCs in the early-type galaxies have best fit average formation epochs of z = 3.4 and z = 7.4 respectively. Similarly, the MRGC and MPGC subpopulations of the Milky Way correspond to z = 2.4 and z = 7.4, if the GCs formed in the Milky Way with its current stellar mass.

These formation epochs assume that both GC subpopulations formed within the host galaxy with the mass that it has today (i.e. the GCs formed in-situ within the host galaxy, and the galaxy has not grown in stellar mass after the GCs formed). However, studies of compact, quiescent galaxies at high redshift have concluded that they have grown in mass by a factor of several due to the merger/accretion of lower mass galaxies (Bezanson et al. 2009; Marchesini et al. 2014; Ownsworth et al. 2014; Stefanon et al. 2015). Thus if GCs have formed in-situ, we must consider the mass of the host galaxy at the time of GC formation. Furthermore, GCs may have formed ex-situ, i.e. within a low mass satellite that has been accreted into the halo of the main host galaxy. We consider both the in-situ and accreted origins for GCs in thie discussion below.

Similarities between galaxy stellar properties and MRGCs, e.g. radial density profiles and azimuthal distributions (e.g. Kartha et al. 2014), suggest that a significant fraction of MRGCs formed in-situ within the host galaxy where they now reside. The formation site for MPGCs is less clear. They have more extended radial density profiles than the galaxy starlight indicating a significant contribution from accretion. However, their inner radial metallicity gradients are similar to those of the MRGCs (Harris 2009; Forbes et al. 2011; Pastorello et al. 2015), suggesting that some MPGCs may have also formed in-situ within the same host galaxy as the MRGCs.

Accretion of low mass satellites, and their GCs, is thought to be particularly important in the two-phase formation of massive galaxies (e.g. Oser et al. 2012). The accretion process is expected to be fairly self-similar, with a typical accreted satellite mass having a mass some 10 per cent of its host galaxy (Stewart et al. 2008; Oser et al. 2012; Hirschmann et al. 2015). For our sample of early-type galaxies with a mean mass of log M_* = 11.2, this implies that the accreted satellite mass could be as high as log M_* = 10.2 $M_\odot$ (similar to the mass of M33). We do not expect many MRGCs to be accreted since galaxies with log $M_* < 10.2$ are increasingly unimodal, and dominated by MPGCs (Forbes 2005).

For the Milky Way a satellite galaxy of mass a few 10^9 $M_\odot$ would be more typical. This is similar to the mass of the Sgr dwarf (Niederste-Ostholt et al. 2010), and the recent findings of D'Abrusco et al. (2015) for accreted substructures in GC systems. We note that surviving dwarf galaxies below this mass host very few GCs, e.g. the WLM galaxy with a baryonic mass mass of 10^8 $M_\odot$ (Leaman et al. 2012) hosts only a single metal-poor GC.

In Figure 2 we illustrate the inferred formation epochs for an in-situ or accreted origin for the GCs in our early-type galaxy sample. The two red and blue curved bands show the formation epochs of the MRGC and MPGC subpopulations, derived from the best fit of their mean metallicities to the mass-metallicity relation (Eq. 2), while allowing the host galaxy mass to be a fraction of today's mass. The shaded regions represent the error on the mean and a possible systematic uncertainty of ±0.2 dex.

We show the predicted stellar growth of a galaxy with log $M_* \sim 11.2$ (i.e. the mean mass of our sample), and a galaxy with 10 per cent of that mass today, to represent a typical accreted satellite for our sample of massive early-type galaxies. We label these curves 'in-situ' and 'accreted' respectively to represent the stellar mass growth of the main host galaxy and a typical satellite with look-back time. These curves come from Behroozi et al. (2013), who compared the merger trees of simulated dark matter halos from z = 8 to z = 0 with observations of the star formation efficiency and the stellar mass function.

The in-situ growth line intersects the MRGC curve at log $M_* \sim 10.6$, suggesting a host galaxy mass for MRGC formation some 4 times less than today. It corresponds to a formation epoch of z = 2.9 or a look-back age of 11.5 Gyr. We note that if instead of the Behroozi et al. relation, we had adjusted the observed linear relation of Ownsworth et al. (2014) from their stellar mass of log M_* = 11.56 to

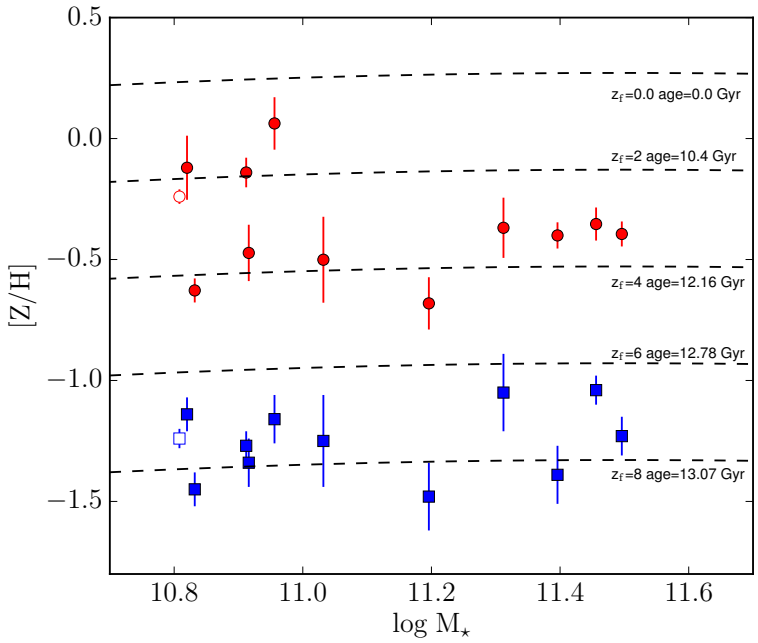

Figure 1. Evolving mass-metallicity relations. The solid red circles and blue squares show, respectively, the average metallicities for the MRGC and MPGC subpopulations in 11 early-type galaxies from the SLUGGS survey. The error bars represent the error on the mean. The open red and blue points represent the MRGCs and MPGCs for the Milky Way. The dashed black lines show the evolving mass-metallicity relations using Eq. 2 (see text for details), and are labelled with the associated formation redshift and look-back age.

match our stellar mass, and used their stellar mass growth from redshifts z = 0.3 to z = 3, it would result in only a small shift in the inferred formation redshift of MRGCs to z ∼ 2.8. This gives us some confidence in the robustness of our results. MPGCs that form in-situ within the main host galaxy had a mean formation epoch of z = 5.9 (12.8 Gyr) and formed in a galaxy 1/50th of today's mass.

For MPGCs that were accreted, the accreted satellite growth line intersects the MPGC curve at log M_* ∼ 8.8, suggesting that a typical satellite was 1/25th of today's mass when MPGCs formed. The corresponding formation epoch for these accreted MPGCs is 4.8 (12.5 Gyr). Figure 2 suggests that any accreted MRGCs would have a mean formation epoch of z = 2.3 (10.8 Gyr), but we expect such MRGCs to be a minor contribution to the in-situ formed MRGCs.

Figure 2 also shows a shaded region representing the epoch of hydrogen reionisation (Robertson et al. 2015). Several GC formation models invoke reionisation as the mechanism to terminate the formation of MPGCs and hence provide a metallicity and temporal gap before MRGC formation occurs. Although the onset of reionisation is still poorly defined, the epoch of instantaneous reionisation inferred from Planck data is z = 8.8 and a variety of different observations indicate that reionisation had essentially ended by z = 6 (see Robertson et al. 2015 for a summary). The figure shows that for our early-type galaxy sample, only MPGCs that form in host galaxies with mass log $M_* \geqslant 9.5$ are affected by reionisation. Below this galaxy mass, a process other than reionisation is needed to establish the distinct mean metallicities observed in MPGC and MRGC subpopulations. A dependence of the typical accreted satellite mass with redshift (e.g. Muratov & Gnedin 2010) is one possible mechanism.

We have performed a similar analysis for the Milky Way GC system. Using the mean metallicity of the Milky Way's MRGC and MPGCs (Table 1) and assuming that a Behroozi et al. (2013) mass growth history for a stellar mass log M_* = 10.8 today is applicable to the Milky Way, we find formation epochs of z = 2.2 (10.7 Gyr) and 5.5 (12.7 Gyr) for in-situ formed MRGCs and MPGCs respectively. For MRGCs and MPGCs accreted from satellites of mass 10 per cent of the Milky Way, the formation epochs are z = 1.8 (10 Gyr) and z = 4.1 (12.2 Gyr) respectively.

A comparison of our findings with cosmological predictions (Section 2) and observations of the Milky Way's GC system (Section 3) are given in Table 2, in which we list the mean look-back ages (or a range if mean ages are not available) and corresponding redshifts. Our findings are discussed in the next section.

Our mean ages are potentially affected by a number of systematic effects, which dominate over any error on the mean value. These include the absolute [O/H] metallicity scale, bias in our spectroscopic metallicities, variations in the colour to metallicity conversion, and instrinsic scatter in $[\alpha/Fe]$ ratios. We conservatively estimate the combined systematic uncertainty to be less than ±0.2 dex. The corresponding uncertainty in the formation epoch from the systematic effects results in a redshift uncertainty of ± 1. In terms of age, the systematic uncertainty is up to +0.6, −1.2 Gyr for the MRGCs which have a mean age of 11.5 Gyr. For the MPGCs, the systematic uncertainty is +0.2, −0.3 for in-situ formed MPGCs with a mean age of 12.8 Gyr, and +0.2, −0.4 for MPGCs formed in satellites with a mean age of 12.5 Gyr. As well as increasing the sample size, future efforts to apply this method should be directed at reducing possible systematic effects.

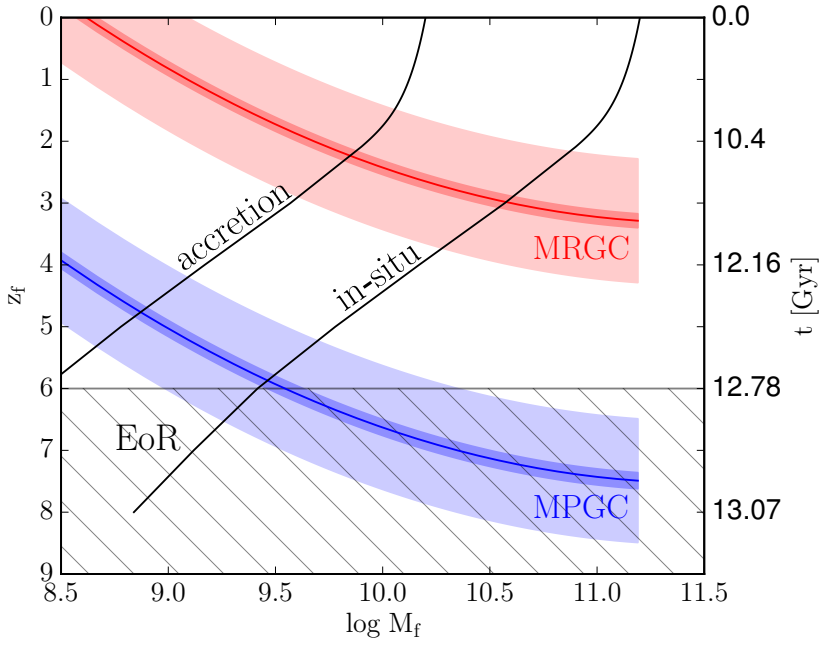

Figure 2. Formation epoch for MPGCs and MRGCs. The formation epoch is shown as a function of galaxy stellar mass at formation. The blue and red curved bands show the MPGC and MRGC formation epochs for a range of galaxy formation mass ranging from a host galaxy with the mean stellar mass of our sample (i.e. log $M_* = 11.2$). The dark shaded regions show the error on the mean metallicity, and the light shaded regions show the possible range of systematic uncertainty in the mean metallicity. The grey hashed region at the bottom of the plot shows the epoch of reionisation (EoR). The curved black solid lines show the predicted stellar mass growth from z = 8 by Behroozi et al. (2013). The 'in-situ' curve shows the growth of a log $M_* = 11.2$ galaxy today, while the 'accreted' curve shows the growth of a satellite of mass 10 per cent that of our sample, i.e. log $M_* = 10.2$. In the simplified picture that MRGC form in-situ within the main host galaxy, and MPGCs are accreted from satellites, with implied formation epochs of z = 2.9 (11.5 Gyr) and z = 4.8 (12.5 Gyr) respectively. In reality, MPGCs may have a significant in-situ formed component, and accretion may contribute some MRGCs, thus increasing the inferred age difference between the two GC subpopulations.

Table 2. Age and redshift of formation for GC subpopulations. Predictions from cosmological models, Milky Way observations and the results from this work on 11 early-type galaxies and the Milky Way. We assume a Bennett et al. (2014) cosmology.

Author	MPGC Gyr (z)	MRGC Gyr (z)	ΔAge Gyr
Beasley	12.7 (5.8)	10.2 (1.9)	2.5
Santos	>13.0 (>7)	>11.5 (>3)	<1.5
Bekki	12.7 (5.7)	12.3 (4.3)	0.4
Griffen	13.4-13.6 (13-22)	7-13.3 (0.8-11)	0.1-6.6
Tonini	11.5-12.2 (3-4)	10.4 (2)	1.1-1.8
Li	12.2-12.8 (4-6)	7.8-12.2 (1-4)	0-5
Katz†	13.0-13.4 (7-12)	10.4 (2)	2.6-3.0
Corbett	13.1 (9)	–	–
Trenti	13.2 (9.3)	–	–
MW ages	12.5-12.8 (5-6.1)	11.0-12.8 (2.4-6.1)	0-1.5
11 ETGs	12.5-12.8 (4.8-5.9)	11.5 (2.9)	1.0-1.3
MW	12.2-12.7 (4.1-5.5)	10.7 (2.2)	1.5-2.0

† predictions for GCs in Milky Way type galaxies.

7 DISCUSSION AND CONCLUSIONS

The mass-metallicity relation for massive galaxies is a strong function of redshift and only a weak function of galaxy mass. Here we exploit this fact, and new measurements of the mean metallicity in 11 massive early-type galaxies from the SLUGGS survey, to estimate the mean formation epoch of metal-rich (MR) and metal-poor (MP) globular clusters (GCs). We find more scatter in the mean metallicity of the MRGCs than for the MPGCs.

We infer a formation epoch for MRGCs of z = 2.9 and hence a mean age of 11.5 Gyr. We expect the contribution of (slightly younger) MRGCs formed in satellites and later accreted into the halos of early-type galaxies to be small. Our MRGC mean age is broadly in line with most cosmological model predictions for GC formation. Although we find a younger age than the mean of 12.3 Gyr predicted by Bekki et al. (2008), their simulations suggested that a wide range of MRGC ages are possible. Using a similar method for the Milky Way we find a mean age of 10.7 Gyr for the MRGCs. This is somewhat younger than the MRGCs associated with the bulge of the Milky Way.

We infer mean ages for the MPGCs to be 12.5 Gyr if they all accreted from satellites and 12.8 Gyr if they are all formed in-situ within the main host galaxy. Our MPGC mean age limits of 12.5–12.9 Gyr are consistent with predictions from several cosmological models. However, our results disfavour models that predict very early MPGC formation (ages of $\geqslant$ 13.2 Gyr and z $\geqslant$ 9) in dark matter minihalos. For the MPGCs of the Milky Way we infer mean age limits of between 12.2–12.7 Gyr, which is consistent with current observational results. The MPGC mean ages from our

work, and Milky Way observations, suggest that MPGCs continued to form long after the end of reionisation, casting doubt on simulations that invoke reionisation to explain the observed metallicity differences between the two GC subpopulations, or indeed, invoke GCs as the main source of reionisation.

We note that the only cosmological model that is consistent with *both* our MPGC and MRGC mean ages is that of Li & Gnedin (2014). In their model the vast bulk of GCs form after reionisation has ended, and metallicity bimodality is established by MPGCs that form at high redshift, i.e. z $\sim$ 4–6 (12.2–12.8 Gyr) and MRGCs which peak around z $\sim$ 3–4 (11.5–12.2 Gyr) but can continue to form to z $\sim$ 1 (7.8 Gyr).

Historically it has been very difficult to verify directly an age difference in extragalactic GC subpopulations, and hence whether they formed in independent formation episodes. Here we infer a mean age difference between the MPGC and MRGC subpopulations in masive early-type galaxies of between 1.0 and 1.3 Gyr. This age difference is somewhat smaller than the mean difference predicted by Beasley et al. (2002) and larger than that of Bekki et al. (2008). For the Milky Way we infer a difference of 1.5–2 Gyr. The prediction from the Katz & Ricotti (2014) simulation of Milky Way like galaxies is 2.6–3.0 Gyr. An age difference of 1.5 Gyr was measured for the Milky Way's GC system by VandenBergh et al. (2013), while no measurable age difference was found by Marin-Franch et al. (2009).

Future high resolution hydrodynamical simulations in the relevant redshift range of $2 < z < 7$ could reveal important clues regarding the relative roles of in-situ and ex-situ (accreted) GCs. Additional work is also needed on the observational side to better understand systematic uncertainties in applying an evolving mass-metallicity relation to determine the formation epoch of GCs. Nevertheless larger samples of GCs over a range of host galaxy masses offer the potential for interesting constraints on the mean age of GCs and galaxy assembly in general.

8 ACKNOWLEDGEMENTS

We thank L. Cortese and L. Spitler for useful discussions. DAF thanks the ARC for financial support via DP130100388. This work was supported by NSF grant AST-1211995. Finally, we thank the referee for a prompt report and several useful suggestions to improve the paper.

9 REFERENCES

Bailin J., Harris W. E., 2009, ApJ, 695, 1082
Baistan N., Cabrera-Ziri I., Davies B., Larsen S. S., 2013, MNRAS, 436, 2852
Beasley M. A., Baugh C. M., Forbes D. A., Sharples R. M., Frenk C. S., 2002, MNRAS, 333, 383
Bedin L. R., Salaris M., Piotto G., Anderson J., King I. R., Cassisi S., 2009, ApJ, 697, 965
Behroozi P. S., Wechsler R. H., Conroy C., 2013, ApJ, 770, 57
Bekki K., Yahagi H., Nagashima M., Forbes D. A., 2008, MNRAS, 387, 1131
Bennett C. L., Larson D., Weiland J. L., Hinshaw G., 2014, ApJ, 794, 135
Bezanson R., van Dokkum P. G., Tal T., Marchesini D., Kriek M., Franx M., Coppi P., 2009, ApJ, 697, 1290
Boley A. C., Lake G., Read J., Teyssier R., 2009, ApJ, 706, L192
Brodie J. P., Strader J., 2006, ARA&A, 44, 193
Brodie J. P., et al., 2014, ApJ, 796, 52
Bromm V., Clarke C. J., 2002, ApJ, 566, L1
Corbett Moran C., Teyssier R., Lake G., 2014, MNRAS, 442, 2826
D'Abrusco R., Fabbiano G., Zezas A., 2015, ApJ, 805, 26
Erb D. K., Shapley A. E., Pettini M., Steidel C. C., Reddy N. A., Adelberger K. L., 2006, ApJ, 644, 813
Forbes D. A., 2005, ApJ, 635, L137
Forbes D. A., Bridges T., 2010, MNRAS, 404, 1203
Forbes D. A., Spitler L. R., Strader J., Romanowsky A. J., Brodie J. P., Foster C., 2011, MNRAS, 413, 2943
Garcia-Berro E., Torres S., Althaus L. G., Miller Bertolami M. M., 2014, A&A, 571, A56
Griffen B. F., Drinkwater M. J., Thomas P. A., Helly J. C., Pimbblet K. A., 2010, MNRAS, 405, 375
Hansen B. M. S., et al., 2013, Natur, 500, 51
Harris W. E., 1996, AJ, 112, 1487
Harris W. E., 2009, ApJ, 703, 939
Hirschmann M., Naab T., Ostriker J. P., Forbes D. A., Duc P.-A., Davé R., Oser L., Karabal E., 2015, MNRAS, 449, 528
Jarrett T. H., Chester T., Cutri R., Schneider S., Skrutskie M., Huchra J. P., 2000, AJ, 119, 2498
Kacprzak G. G., et al., 2015, ApJ, 802, L26
Kartha S. S., Forbes D. A., Spitler L. R., Romanowsky A. J., Arnold J. A., Brodie J. P., 2014, MNRAS, 437, 273
Katz H., Ricotti M., 2014, MNRAS, 444, 2377
Kewley L. J., Ellison S. L., 2008, ApJ, 681, 1183
Kruijssen J. M. D., 2014, CQGra, 31, 244006
Lada C. J., Lada E. A., 2003, ARA&A, 41, 57
Leaman R., et al., 2012, ApJ, 750, 33
Li H., Gnedin O. Y., 2014, ApJ, 796, 10
Ma X., et al. 2015, arXiv:1504.02097
Mannucci F., et al., 2009, MNRAS, 398, 1915
Marchesini D., et al., 2014, ApJ, 794, 65
Marin-Franch A., et al., 2009, ApJ, 694, 1498
McMillan P. J., 2011, MNRAS, 414, 2446
Muratove A. L., Gnedin O. Y., 2010, ApJ, 718, 1266
Pastorello N., Forbes D. A., Foster C., Brodie J. P., Usher C., Romanowsky A. J., Strader J., Arnold J. A., 2014, MNRAS, 442, 1003
Niederste-Ostholt M., Belokurov V., Evans N. W., Koposov S., Gieles M., Irwin M. J., 2010, MNRAS, 408, L66
Ownsworth J. R., Conselice C. J., Mortlock A., Hartley W. G., Almaini O., Duncan K., Mundy C. J., 2014, MNRAS, 445, 2198
Oser L., Naab T., Ostriker J. P., Johansson P. H., 2012, ApJ, 744, 63
Pastorello N., et al. 2015, arXiv:1505.04795
Peng E. W., et al., 2006, ApJ, 639, 838
Piotto G., et al., 2007, ApJ, 661, L53
Pritzl B. J., Venn K. A., Irwin M., 2005, AJ, 130, 2140
Puzia T. H., Kissler-Patig M., Thomas D., Maraston C., Saglia R. P., Bender R., Goudfrooij P., Hempel M., 2005, A&A, 439, 997

Robertson B. E., Ellis R. S., Furlanetto S. R., Dunlop J. S., 2015, ApJ, 802, L19
Sanders R. L., et al., 2015, ApJ, 799, 138
Santos M. R., 2003, egcs.conf, 348
Shapiro K. L., Genzel R., Förster Schreiber N. M., 2010, MNRAS, 403, L36
Spitler L. R., 2010, MNRAS, 406, 1125
Spitler L. R., Romanowsky A. J., Diemand J., Strader J., Forbes D. A., Moore B., Brodie J. P., 2012, MNRAS, 423, 2177
Springel V., et al., 2005, Natur, 435, 629
Strader J., Brodie J. P., Cenarro A. J., Beasley M. A., Forbes D. A., 2005, AJ, 130, 1315
Strader J., Smith G. H., 2008, AJ, 136, 1828
Stefanon M., et al., 2015, ApJ, 803, 11
Stewart K. R., Bullock J. S., Wechsler R. H., Maller A. H., Zentner A. R., 2008, ApJ, 683, 597
Thomas D., Maraston C., Bender R., 2003, MNRAS, 339, 897
Tonini C., 2013, ApJ, 762, 39
Tremonti C. A., et al., 2004, ApJ, 613, 898
Trenti M., Perna R., Jimenez R., 2015, ApJ, 802, 103
Usher C., et al., 2012, MNRAS, 426, 1475
Usher C., et al., 2015, MNRAS, 446, 369
VandenBerg D. A., Brogaard K., Leaman R., Casagrande L., 2013, ApJ, 775, 134
Vazdekis A., Cenarro A. J., Gorgas J., Cardiel N., Peletier R. F., 2003, MNRAS, 340, 1317
Wright E. L., 2006, PASP, 118, 1711